

Controlled thermally-driven mass transport in carbon nanotubes using carbon hoops

Yaolong Li(李耀隆), Songyuan Li(李松远), Meifen Wang(王美芬), and Renliang Zhang(张任良)

Citation: Chin. Phys. B, 2024, 33 (**4**): 046101. DOI: 10.1088/1674-1056/ad14ff
Journal homepage: http://cpb.iphy.ac.cn; http://iopscience.iop.org/cpb

What follows is a list of articles you may be interested in

Molecular dynamics study of primary radiation damage in TiVTa concentrated solid-solution alloy

Yong-Peng Zhao(赵永鹏), Yan-Kun Dou(豆艳坤), Xin-Fu He(贺新福), Han Cao(曹晗),Lin-Feng Wang(王林枫), Hui-Qiu Deng(邓辉球), and Wen Yang(杨文)
Chin. Phys. B, 2024, 33 (**3**): 036104. DOI: 10.1088/1674-1056/ad0146

Electronic effects on radiation damage in α-iron: A molecular dynamics study

Lin Jiang(江林), Min Li(李敏), Bao-Qin Fu(付宝勤), Jie-Chao Cui(崔节超), and Qing Hou(侯氢)
Chin. Phys. B, 2024, 33 (**3**): 036103. DOI: 10.1088/1674-1056/ad0ec4

Anelasticity to plasticity transition in a model two-dimensional amorphous solid

Baoshuang Shang(尚宝双)
Chin. Phys. B, 2024, 33 (**1**): 016102. DOI: 10.1088/1674-1056/acf82c

Universal basis underlying temperature, pressure and size induced dynamical evolution in metallic glass-forming liquids

H P Zhang(张华平), B B Fan(范蓓蓓), J Q Wu(吴佳琦), and M Z Li(李茂枝)
Chin. Phys. B, 2024, 33 (**1**): 016101. DOI: 10.1088/1674-1056/acf994

Classification and structural characteristics of amorphous materials based on interpretable deep learning

Jiamei Cui(崔佳梅), Yunjie Li(李韵洁), Cai Zhao(赵偲), and Wen Zheng(郑文)
Chin. Phys. B, 2023, 32 (**9**): 096101. DOI: 10.1088/1674-1056/acd7d0

SPECIAL TOPIC — Heat conduction and its related interdisciplinary areas

Controlled thermally-driven mass transport in carbon nanotubes using carbon hoops

Yaolong Li(李耀隆)[1,2], Songyuan Li(李松远)[1,2], Meifen Wang(王美芬)[1,2], and Renliang Zhang(张任良)[1,2,†]

[1] *Hebei Key Laboratory of Mechanical Reliability for Heavy Equipment and Large Structures, Yanshan University, Qinhuangdao* 066004, *China*
[2] *School of Civil Engineering and Mechanics, Yanshan University, Qinhuangdao* 066004, *China*

(Received 1 September 2023; revised manuscript received 6 December 2023; accepted manuscript online 13 December 2023)

Controlling mass transportation using intrinsic mechanisms is a challenging topic in nanotechnology. Herein, we employ molecular dynamics simulations to investigate the mass transport inside carbon nanotubes (CNT) with temperature gradients, specifically the effects of adding a static carbon hoop to the outside of a CNT on the transport of a nanomotor inside the CNT. We reveal that the underlying mechanism is the uneven potential energy created by the hoops, i.e., the hoop outside the CNT forms potential energy barriers or wells that affect mass transport inside the CNT. This fundamental control of directional mass transportation may lead to promising routes for nanoscale actuation and energy conversion.

Keywords: molecular dynamics, thermal drive, nanotube hoop, mass transport

PACS: 61.46.Fg, 31.15.xv, 31.15.at **DOI:** 10.1088/1674-1056/ad14ff

1. Introduction

Controlling mass transportation enables a wide range of applications,[1–8] such as the design and fabrication of nanoelectromechanical systems,[9–13] particle separation,[14,15] drug delivery,[16,17] and energy conversion.[18,19] There are many ways to control mass transportation, such as the simplest transmission method of gravity, the impact of channels geometric,[20] and defects[21] on water transport behavior, phonon induction that causes the movement of water nanodroplets[22] and external excitation that causes impact response.[23] In addition, thermophoresis is also a simple way to induce mass transportation in small molecules and particles by generating a force using a temperature gradient.

Low dimensional materials such as carbon nanotubes (CNT) and graphene are widely used in nanomechanical systems due to their excellent mechanical, electrical properties and adjustable excellent thermodynamic properties.[24–26] Recently, numerous studies[27–29] have reported that thermal gradients can drive mass transport along the tube of a CNT. Furthermore, these studies have theoretically and experimentally demonstrated mass can be transported by thermophoresis in fluids[30,31] and solids.[32] The mass generally transports in the direction of decreasing temperature,[27,28,33] and the driving force is mainly attributed to the thermally induced edge force and the interlayer attraction force.[34,35] Moreover, molecular dynamics (MD) simulations are used to show that mass transportation can occur in the direction of temperature gradient reduction in solid–solid interfaces.[36] However, it remains a challenge to control mass transportation using an intrinsic mechanism.

Considering the requirements of practical applications, it is necessary to develop effective methods to manipulate mass transportation without relying on extrinsic power sources or complicated dynamic control systems. Herein, we use MD simulations to reveal that their mass transportation can be controlled by an interlayer potential. Specifically, in single-walled carbon nanotubes with an axial temperature gradient, the confined nanomotor will move spontaneously in the direction of decreasing temperature, and the behavior is affected by a physical hoop that is confined outside the nanotube. Under different conditions, the hoop generates a potential energy barrier or a potential well, resulting in an intrinsic mechanism for manipulating nanomotor motion, which has general implications for nanoscale actuation and energy conversion.

2. Computational methods

As illustrated in Fig. 1(a), the simulated structure consists of a hoop (a short outer CNT), a CNT substrate (a long intermediate carbon nanotube), and a nanomotor (a short inner CNT). The hoop is placed at the center of the CNT substrate, and the nanomotor is initially placed on the left side of the CNT substrate. The CNT substrate has a chirality of (10, 10) and a length of 60.4 nm for all simulations. The hoop is a shorter CNT with a chirality of (15, 15). The length of the hoop is l_{h}, and the distance between the mass center of the hoop and the left end of the CNT substrate is L. The nanomotor is also a short CNT with a chirality of (6, 6) or (5, 5), with corresponding diameters of 0.81 nm and 0.68 nm. The length of the nanomotor is 2.46 nm, and the initial distance between the mass center of the nanomotor and the left end of the CNT

†Corresponding author. E-mail: zhrleo@ysu.edu.cn

© 2024 Chinese Physical Society and IOP Publishing Ltd

substrate is approximately 11.07 nm. The outermost carbon atoms at the ends of the CNT substrate are fixed to prevent atoms from vibrating, and the centers of mass of the hoop and the nanomotor are constrained in the z direction.

In the presence of a temperature gradient along the CNT substrate (high temperature on the left end and low temperature on the right end), the nanomotor movement is demonstrated using the MD method, performed by a large-scale atomic/molecular massively parallel simulator.[37] The in-plane carbon–carbon bond interactions are described by the adaptive intermolecular reactive empirical bond order potential[38] and the interlayer van der Waals (vdW) interactions are described by a Lennard–Jones (LJ) potential (with potential well $\varepsilon = 2.968$ meV, an equilibrium distance $\sigma_{\mathrm{OC}} = 3.407$ Å, and cutoff distance $r_{\mathrm{c}} = 8.5$ Å), as described in previous studies.[4,5,39]

In the first step of the simulation, the whole system is equilibrated for 100 ps at 300 K using an NVT (canonical) ensemble to eliminate the possible bias caused by the corrugated potential profile of the discrete atomic structures. The second step is to impose specified temperatures on the two ends portions of the substrate respectively by the Nose–Hoover thermostat, and reach a steady temperature profile after 100 ps to obtain the temperature gradient (∇T) of the CNT substrate. In the third step, an NVE ensemble is adopted, which initiates as soon as the constraint on the nanomotor's center of mass is released. Then, the nanomotor moves along the CNT substrate.

3. Result and discussions

Because of the thermophoretic force,[27,39] the nanomotor moves from the high-temperature region to the low-temperature region, that is, from the left side to the right side of the CNT substrate. The total vdW force acting on the nanomotor can be calculated by summing all the forces corresponding to the LJ potential between the carbon atoms of the nanomotor and the carbon atoms of the substrate and hoop. When the nanomotor starts to move (far away from the hoop), the vdW force acting on the nanomotor is only applied by the CNT substrate, and the component of the vdW force along the direction of motion is the thermophoretic force. In contrast, when the nanomotor moves close to the hoop, the vdW force acting on the nanomotor is applied not only by the CNT substrate but also by the hoop, which affects the axial movement of the nanomotor along the CNT substrate.

To demonstrate this effect, Fig. 1(b) plots the component of the vdW force acting on the nanomotor in the direction of motion as a function of the distance from the nanomotor to the hoop. Initially, the nanomotor is placed on the left side of the hoop, approximately 4.92 nm from the center of mass of the hoop. The displacement of the nanomotor along the CNT substrate is accurately controlled as in Ref. [40], with displacement steps of 0.05 nm. At each position, after relaxation to equilibrium, we record the instantaneous tangential force acting on the nanomotor at each time step. After 50 ps statistical averaging, the component of the vdW force acting on the nanomotor in the direction of motion can be obtained. As shown in Fig. 1(b), when the nanomotor is far from the hoop, the nanomotor cannot feel the force exerted by the hoop, and the vdW force is only composed of the thermophoretic force (the existence of static friction). When the nanomotor moves toward the hoop, the hoop has a stronger effect on the nanomotor, which varies with the diameter of the nanomotor. For a nanomotor with a larger diameter, the force prevents the nanomotor from moving toward the hoop, whereas a nanomotor with a smaller diameter can move toward the hoop. As the nanomotor approaches the hoop, the vdW force on the nanometer increases, but the force becomes zero when the nanomotor reaches the center of the hoop. Likewise, as the nanomotor moves just beyond the center point of the hoop and continues to move to the right edge of the hoop, the force on the nanomotor increases to the maximum. For the large-diameter nanomotor, the effect of the force is to push the nanomotor away from the hoop. For the small-diameter nanomotor, the effect of the force is to prevent the nanomotor from leaving the hoop. As the nanomotor continues to move to the right, the force exerted on the nanomotor by the hoop gradually decreases, until only the thermophoretic force is acting on the nanomotor. In short, the hoop attracts or repels the nanomotor depending on the diameter of the nanomotor. When the diameter of the nanomotor is sufficiently large, the system exhibits repulsion, and when the diameter of the

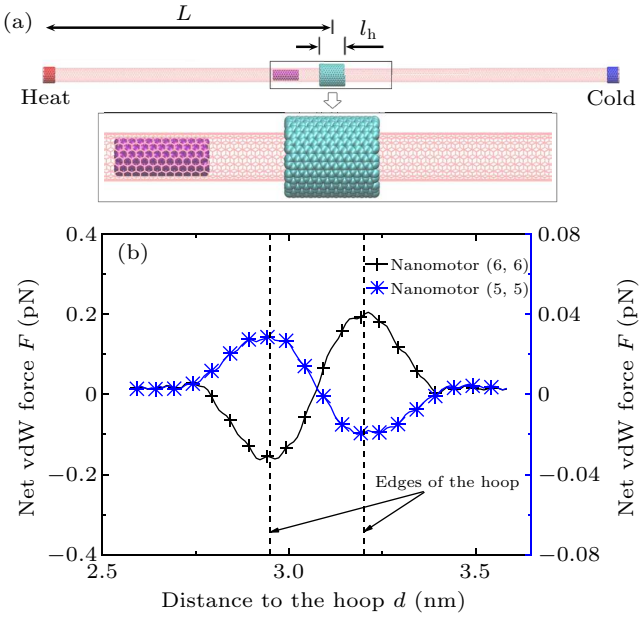


Fig. 1. (a) Schematic of the simulation system. A 2.46-nm-long hoop is positioned outside the carbon nanotube and a 2.46-nm-long nanomotor is placed inside the carbon nanotube. (b) Net vdW force acting on the nanotube nanomotor as a function of the distance from the nanomotor to the hoop. Dashed lines mark the location of the edges of the hoop.

nanomotor is sufficiently small, it exhibits attraction. The hoop effect demonstrated in Fig. 1(b) is the physical origin of the proposed approach, which demonstrates the controlled movement of the nanomotor along the CNT substrate with different temperature gradients by placing hoops at different positions and spacings.

As an example of the hoop effect, we study the effects of hoop position and length on the nanomotor motion. Additionally, we study the effects of the temperature gradient and nanomotor diameter on the nanomotor motion, particularly in the presence of the hoop. We employ a model system (like that shown in Fig. 1(a)) to simplify the system. The parameters (∇T, l_h, L, and nanomotor diameter) for seven cases of nanomotor movement are shown in Table 1. For different cases, the displacement of the nanomotor's mass center with time is shown in Fig. 2.

Table 1. Simulation parameters for seven cases.

Case	∇T (K/nm)	l_h (nm)	L (nm)	Diameter (nm)
1	2.18	2.46	30.74	0.81
2	2.18	2.46	50.42	0.81
3	2.18	4.92	50.42	0.81
4	4.19	2.46	30.74	0.81
5	0.93	2.46	50.42	0.81
6	2.18	2.46	30.74	0.68
7	2.18	4.92	50.42	0.68

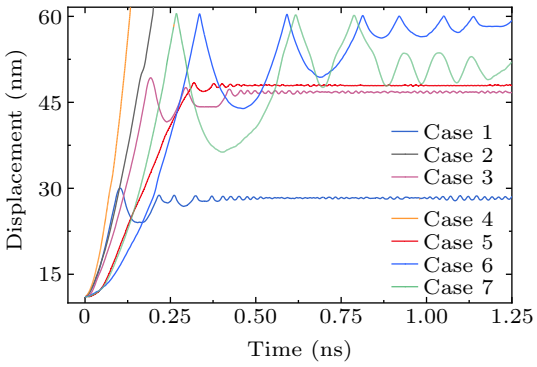


Fig. 2. Time evolution of the nanomotor's center of mass position for the seven cases.

From Fig. 2, the nanomotor is initially driven by thermophoretic force and moves toward the low-temperature region, which is consistent with the previous experimental study[27] and numerical simulation study.[32,39] Considering the same temperature gradient ($\nabla T = 2.18$ K/nm), when the hoop is placed in the middle ($L = 30.74$ nm) of the CNT substrate, the hoop ($l_h = 2.46$ nm) prevents the nanomotor from passing through the hoop (case 1), and when the same hoop is placed on the right side ($L = 50.42$ nm) of the CNT substrate, the nanomotor can break the resistance of the hoop and pass through (case 2). However, if the length of the hoop is doubled ($l_h = 4.92$ nm) and the centroid is placed in the same position on the right side ($L = 50.42$ nm), the nanomotor is prevented from passing through the hoop (case 3).

In the presence of the hoop effect, changing the temperature gradient can also affect the motion of the nanomotor. When the temperature gradient increases from 2.18 K/nm to 4.19 K/nm, the nanomotor can pass through the hoop (case 4) at the middle position ($L = 30.74$ nm), which is not possible in case 1, when the temperature gradient is too low for this hoop distance. When the temperature gradient is reduced from 2.18 K/nm to 0.93 K/nm, the nanomotor cannot pass through the hoop (case 5) at the right end ($L = 50.42$ nm), which is possible in case 2, when the temperature gradient and hoop distance are sufficiently high. Moreover, the hoop effects depend on the relative diameter of the nanomotor. As shown in Fig. 2, for case 1, the nanomotor cannot pass through the hoop, but under the same temperature gradient, with the same hoop size and position, when the diameter of the nanomotor is reduced to 0.68 nm, the nanomotor can pass through the hoop (case 6) but becomes captured or held just beyond the hoop. Similarly, but corresponding to the conditions for case 3 ($\nabla T = 2.18$ K/nm, $l_h = 4.92$ nm, $L = 50.42$ nm), when the diameter of the nanomotor is reduced to 0.68 nm, the nanomotor can break through the hoop, and then nanomotor is pulled back and captured by the hoop (case 7). This is because the hoop can attract and trap the nanomotor with a smaller diameter, depending on the relative thermophoretic force.

In addition to analyzing the vdW force on the nanomotor, to explain the mechanism more clearly, it is helpful to analyze the potential energy of the nanomotor versus its position in carbon nanotubes. We compute the potential energy difference (Ed) for the seven cases, which is defined as the difference in potential energy between the nanomotors with and without hoops, but all other parameters are constant. Figure 3 shows the Ed of the nanomotor along the length of the CNT substrate.

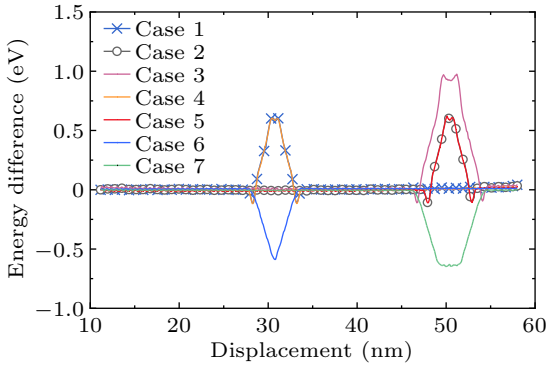


Fig. 3. The energy difference (E_d) of the nanomotor induced by the encounter with the hoop.

When the nanomotor is far away from the hoop, the intermolecular interaction only occurs between the nanomotor and the substrate, and $E_d = 0$. When the nanomotor encounters

the hoop, the E_d changes with the position of the nanomotor, relative to the other case parameters. For the large-diameter nanomotor moving toward the hoop, E_d is positive, which indicates that the hoop presents a potential barrier to the nanomotor and repels it outside the hoop. For the small-diameter nanomotor moving toward the hoop, E_d is negative, which indicates that the hoop presents a potential well and attracts it inside the hoop. Moreover, when the mass center of the nanomotor coincides with the mass center of the hoop, the E_d is the largest, and the maximum value is related to the length of the hoop. For large-diameter nanomotors, when the hoop length is short, the maximum E_d is 0.00242 eV, and when the hoop length is doubled, the maximum E_d is 0.00374 eV. For small-diameter nanomotors, when the hoop length is short, the maximum E_d is -0.00280 eV, while when the hoop length is long, the maximum E_d is -0.00304 eV.

In other words, when the relative diameter of the nanomotor is sufficiently large, the hoop serves as an energy barrier and applies additional force to repel the nanomotor. When the relative diameter of the nanomotor is sufficiently small, the hoop serves as an energy potential well and applies additional force to attract the nanomotor. Additionally, the potential well and barrier increase with increasing hoop length.

The simulation results show that when the nanomotor moves in a single-walled carbon nanotube with a temperature gradient, a hoop outside the tube can affect the motion characteristics of the nanomotor, i.e., the potential energy of the nanomotor is different near the hoop. This implies that such a potential difference can be exploited during the nanomotor transformation between two states. For example, a carbon nanotube with a hoop can be a structural element that can also be used as a store and release of energy in a device. Furthermore, the value of the potential well and the range of the plateau region can be tuned by varying the hoop length, which in turn can be used to control the movement of the nanomotor. Notably, the ability of the hoops to capture the nanomotor (and potentially other molecules and particles) may support applications in the fields of energy and medicine.

4. Conclusion

The presence of the hoop causes a change in the local potential energy of the CNT, which affects the transport behavior of the nanomotor when it moves to this position. The hoop effect is related to the relative diameter of the nanomotor, the length of the hoop, and the temperature gradient of the CNT substrate. According to this effect, we can control the movement of the nanomotor by changing the position of the hoop, number of hoops, hoop spacing, and relative size of the nanomotor for a given temperature gradient (or the temperature gradient can be dynamic). Finally, this study provides additional theoretical insight for mechanical design and material transport based on CNTs in nanoengineering.

Acknowledgments

Project supported by the Doctoral Fund of Yanshan University (Grant No. B919), the Program of Independent Research for Young Teachers of Yanshan University (Grant No. 020000534), and the S&T Program of Hebei Province of China (Grant No. QN2016123). The authors thank the High Performance Computing and Data Center, College of Civil Engineering and Mechanics of Yanshan University.

References

[1] Holt J K, Park H G, Wang Y, Stadermann M, Artyukhin A B, Grigoropoulos C P, Noy A and Bakajin O 2006 *Science* **312** 1034
[2] Coluci V R, Timoteo V S and Galvao D S 2009 *Appl. Phys. Lett.* **95** 045503
[3] Zhang R, Di Q, Wang X and Gu C 2010 *J. Hydrodynam.* **22** 366
[4] Chen J, Gao Y, Wang C, Zhang R, Zhao H and Fang H 2015 *J. Phys. Chem. C* **119** 17362
[5] Chang T, Zhang H, Guo Z, Guo X and Gao H 2015 *Phys. Rev. Lett.* **114** 015504
[6] Zhang R, Du G, Wang M, Yu W and Chen J 2019 *J. Stat. Mech. Theroy Exp.* **2019** 063210
[7] Kurupath V P, Kannam S K, Hartkamp R and Sathian S P 2021 *Desalination* **505** 114978
[8] Zhang R, Du G, Wang M and Li S 2022 *J. Nano Res.* **72** 1
[9] Shen C, Brozena A H and Wang Y 2011 *Nanoscale* **3** 503
[10] Santamaría-Holek I, Reguera D and Rubi J M 2013 *J. Phys. Chem. C* **117** 3109
[11] Zhu F, Guo Z and Chang T 2020 *Appl. Mater. Today* **18** 100520
[12] Shen J, Liu G, Han Y and Jin W 2021 *Nat. Rev. Mater.* **6** 294
[13] Cai K, Sun S, Shi J and Qin Q 2021 *Phys. Rev. Appl.* **15** 054017
[14] Puri I K and Ganguly R 2014 *Annu. Rev. Fluid Mech.* **46** 407
[15] Gascoyne P R C and Vykoukal J 2015 *Electrophoresis* **23** 1973
[16] Liu Z, Chen K, Davis C, Sherlock S, Cao Q, Chen X and Dai H 2008 *Cancer Res.* **68** 6652
[17] Nisar A, Afzulpurkar N, Mahaisavariya B and Tuantranont A 2008 *Sens. Actuators B Chem.* **130** 917
[18] Hochbaum A I and Yang P 2010 *Chem. Rev.* **110** 527
[19] Guo Z, Zhang H, Li J, Leng J, Zhang Y and Chang T 2018 *Nanoscale* **10** 4897
[20] Fan W and Chen J 2020 *Phys. Rev. E* **101** 010101
[21] Wang Y and Chen J 2022 *Europhys. Lett.* **139** 51002
[22] Chen J 2020 *J. Phys. Chem. Lett.* **11** 4298
[23] Chen J, Chen S and Gao Y 2017 *Phys. Rev. B* **95** 134301
[24] Wang J and Chen J 2020 *Phys. Rev. E* **101** 042207
[25] Wang Y and Chen J 2021 *Phys. Rev. B* **104** 224306
[26] Yang J, Du W, Wang Y, Wei N and Chen J 2023 *Phys. Rev. B* **108** 144301
[27] Barreiro A, Rurali R, Hernández E R, Moser J, Pichler T, Forró L and Bachtold A 2008 *Science* **320** 775
[28] Schoen P A, Walther J H, Arcidiacono S, Poulikakos D and Koumoutsakos P 2006 *Nano Lett.* **6** 1910
[29] Zambrano H A, Walther J H and Jaffe R L 2009 *J. Chem. Phys.* **131** 241104
[30] Oyarzua E, Walther J H, Megaridis C M, Koumoutsakos P and Zambrano H A 2017 *ACS Nano* **11** 9997
[31] Oyarzua E, Walther J H and Zambrano H A 2018 *Phys. Chem. Chem. Phys.* **20** 3672
[32] Hou Q, Cao B and Guo Z 2009 *Nanotechnology* **20** 495503
[33] Becton M and Wang X 2014 *J. Chem. Theory Comput.* **10** 722
[34] Guo Z, Chang T, Guo X and Gao H 2011 *Phys. Rev. Lett.* **107** 105502
[35] Guo Z, Chang T, Guo X and Gao H 2012 *J. Mech. Phys. Solids* **60** 1676
[36] Leng J, Guo Z, Zhang H, Chang T, Guo X and Gao H 2016 *Nano Lett.* **16** 6396
[37] Plimpton S 1995 *J. Comput. Phys.* **117** 1
[38] Stuart S J, Tutein A B and Harrison J A 2000 *J. Chem. Phys.* **112** 6472
[39] Zhang R, Li S, Li Y and Wang M 2022 *J. Nano Res.* **74** 97
[40] Huang Y, Zhu S and Li T 2014 *Appl. Phys. Lett.* **104** 093102